View metadata, citation and similar papers at core.ac.uk
brought to you by CORE
provided by NASA Technical Reports Server

Response of the Antarctic Stratosphere to Warm Pool El Niño Events in the GEOS CCM

Margaret M. Hurwitz, In-Sun Song, Luke D. Oman, Paul A. Newman, Andrea M. Molod, Stacey M. Frith and **J. Eric Nielsen**

Submitted to Atmospheric Chemistry and Physics, March 2011

A new type of El Niño event has been identified in the last decade. During "warm pool" El Niño (WPEN) events, sea surface temperatures (SSTs) in the central equatorial Pacific are warmer than average. The El Niño signal propagates poleward and upward as large-scale atmospheric waves, causing unusual weather patterns and warming the polar stratosphere. In austral summer, observations show that the Antarctic lower stratosphere is several degrees (K) warmer during WPEN events than during the neutral phase of El Niño/Southern Oscillation (ENSO). Furthermore, the stratospheric response to WPEN events depends of the direction of tropical stratospheric winds: the Antarctic warming is largest when WPEN events are coincident with westward winds in the tropical lower and middle stratosphere i.e., the westward phase of the quasi-biennial oscillation (QBO). Westward winds are associated with enhanced convection in the subtropics, and with increased poleward wave activity.

In this paper, a new formulation of the Goddard Earth Observing System Chemistry-Climate Model, Version 2 (GEOS V2 CCM) is used to substantiate the observed stratospheric response to WPEN events. One simulation is driven by SSTs typical of a WPEN event, while another simulation is driven by ENSO neutral SSTs; both represent a present-day climate. Differences between the two simulations can be directly attributed to the anomalous WPEN SSTs. During WPEN events, relative to ENSO neutral, the model simulates the observed increase in poleward planetary wave activity in the South Pacific during austral spring, as well as the relative warming of the Antarctic lower stratosphere in austral summer. However, the modeled response to WPEN does not depend on the phase of the QBO. The modeled tropical wind oscillation does not extend far enough into the lower stratosphere and upper troposphere, likely explaining the model's insensitivity to the phase of the QBO during WPEN events.

Response of the Antarctic stratosphere to warm pool El Niño Events in the GEOS CCM

Margaret M. Hurwitz [1, *], In-Sun Song [2], Luke D. Oman [3], Paul A. Newman [3], Andrea M. Molod [4], Stacey M. Frith [5] and J. Eric Nielsen [5]

[1] {NASA Postdoctoral Program, NASA Goddard Space Flight Center, Greenbelt, MD, USA}

[2] {Goddard Earth Sciences and Technology Center (GEST), University of Maryland, Baltimore County, Baltimore, MD, USA}

[3] {NASA Goddard Space Flight Center, Greenbelt, MD, USA}

[4] {Earth System Science Interdisciplinary Center (ESSIC), University of Maryland, College Park, College Park, MD, USA}

[5] {Science Systems and Applications, Inc., Lanham, MD, USA}

[*] {Now at: Goddard Earth Sciences and Technology Center (GEST), University of Maryland, Baltimore County, Baltimore, MD, USA}

Correspondence to: Margaret M. Hurwitz (margaret.m.hurwitz@nasa.gov)

Abstract

A new formulation of the Goddard Earth Observing System Chemistry-Climate Model, Version 2 (GEOS V2 CCM), with an improved general circulation model and an internally generated quasi-biennial oscillation (QBO), is used to investigate the response of the Antarctic stratosphere to (1) warm pool El Niño (WPEN) events and (2) the sensitivity of this response to the phase of the QBO. Two 50-year time-slice simulations are forced by repeating annual cycles of sea surface temperatures and sea ice concentrations composited from observed WPEN and neutral ENSO (ENSON) events. In these simulations, greenhouse gas and ozone-depleting substance concentrations represent the present-day climate. The modelled responses to WPEN, and to the phase of the QBO during WPEN, are compared with NASA's Modern Era Retrospective-Analysis for Research and Applications (MERRA) reanalysis.

WPEN events enhance poleward planetary wave activity in the central South Pacific region during austral spring, leading to relative warming of the Antarctic lower stratosphere in November/December. During the easterly phase of the QBO (QBO-E), the GEOS V2 CCM reproduces the observed 4-5 K warming of the polar region at 50 hPa, in the WPEN simulation relative to ENSON.

In the recent past, the response to WPEN events was sensitive to the phase of the QBO: the enhancement in planetary wave driving and the lower stratospheric warming signal were mainly associated with WPEN events coincident with QBO-E. In the GEOS V2 CCM, however, the Antarctic response to WPEN events is insensitive to the phase of the QBO: the modelled response is always easterly QBO-like. OLR, streamfunction and Rossby wave energy diagnostics are used to show that the modelled QBO does not extend far enough into the lower stratosphere and upper troposphere to modulate convection and thus planetary wave activity in the south central Pacific.

1 Introduction

Recent literature has identified two types of El Niño events. Conventional or "cold tongue" El Niño (CTEN) events are characterized by positive sea surface temperature (SST) anomalies in the eastern equatorial Pacific (Niño 3 region) (Rasmusson and Carpenter, 1982; Kug et al., 2009), while "warm pool" El Niño (WPEN) events are characterized by positive SST anomalies in the central equatorial Pacific (Niño 4 region) (Larkin and Harrison, 2005; Ashok et al., 2007; Kug et al., 2009).

The Northern Hemisphere (NH) stratosphere response to CTEN events is well recognized. El Niño-related warming of the Arctic stratosphere has been identified in both observational (Bronnimann et al., 2004; Free and Seidel, 2009) and modelling studies (Sassi et al., 2004; Manzini et al., 2006; Cagnazzo et al., 2009). This warming is a response to increased planetary wave driving: Garfinkel and Hartmann (2008) showed that the extra-tropical tropospheric teleconnections produced during El Niño events weaken the Arctic vortex, leading to higher stratospheric temperatures during the NH winter season. Furthermore, the phase of the quasi-biennial oscillation (QBO) modulates the stratospheric response to CTEN: The Arctic vortex is weakest in years when CTEN events coincide with the easterly phase of the QBO (Garfinkel and Hartmann, 2007).

Hurwitz et al. (2011) identified a robust response to WPEN in the Southern Hemisphere (SH) spring and summer. By compositing observed WPEN and ENSO neutral (ENSON) events, these authors used meteorological reanalyses to show the poleward extension and increased strength of the South Pacific Convergence Zone SPCZ during WPEN events, as compared with ENSON, in austral spring. This configuration of convective activity in the south Pacific favoured an enhancement of planetary wave activity in the upper troposphere, and on average, higher polar stratospheric temperatures and a weakening of the Antarctic polar jet in austral summer. Analogously to the NH response to CTEN events, the authors found the SH response to WPEN events to be dependent on the phase of the quasi-biennial oscillation (QBO): planetary wave driving was strongest in WPEN years coincident with the easterly phase of the QBO.

While the conclusions reached by Hurwitz et al. (2011) were based on physical arguments, statistically robust, and consistent amongst several reanalysis datasets, the scope of the authors' study was limited by the small number of WPEN events during the satellite era. In particular, the WPEN and easterly QBO composite consisted of just three events. Hurwitz et al. (2011) concluded that simulations forced by repeating WPEN and ENSON boundary conditions would greatly increase the sample size and strengthen their findings. Such simulations require a model with a well-resolved stratosphere, a QBO, and because the stratospheric response to WPEN occurs in austral spring and summer, interactive polar ozone chemistry.

This paper presents the first attempt to simulate the SH stratospheric response to WPEN events. Section 2 describes the atmospheric datasets and time-slice simulations with the Goddard Earth Observing System Chemistry-Climate Model, Version 2 (GEOS V2 CCM) to be analyzed. In Section 3, OLR, tropospheric stationary wave patterns, a Rossby wave source diagnostic, eddy heat flux at 100 hPa and stratospheric temperatures illustrate the observed and modelled responses to WPEN events, as well as modulation of the WPEN response by the QBO. Section 4 provides a summary of the results and a brief discussion.

2 Model and data sources

2.1 Atmospheric datasets

The Modern Era Retrospective-Analysis for Research and Applications (MERRA) is used to calculate streamfunction, eddy heat flux, temperature, wind and planetary wave energy diagnostics for the 1979-2009 period. MERRA is a reanalysis dataset based on an extensive set of satellite observations and on the Goddard Earth Observing System Data Analysis System, Version 5 (GEOS-5)(Bosilovich et al., 2008; Rienecker et al., in preparation). The MERRA reanalysis has vertical coverage up to 0.1 hPa, and for this study, is interpolated to 1.25° x 1.25° horizontal resolution. Hurwitz et al. (2011) showed that the response to WPEN was consistent amongst several meteorological reanalyses, including MERRA.

Zonal winds from the MERRA reanalysis are used to characterize the phase of the QBO. For each year between 1979 and 2009, November/December mean zonal winds at 50 hPa,

between 10°S and 10°N, form a QBO index: QBO easterly years (QBO-E) are identified when the QBO index is less than -2 m s^{-1}; QBO westerly years (QBO-W) are identified when the QBO index is larger than 2 m s^{-1}.

Outgoing longwave radiation (OLR) between 1979 and 2009 is obtained from the NOAA interpolated OLR dataset (Liebmann and Smith, 1996), provided by NOAA/OAR/ESRL Physical Sciences Division, Boulder, CO.

WPEN and ENSON events are identified using SON seasonal mean SST anomalies in the Niño 3 and Niño 4 regions (www.cpc.noaa.gov/data/indices), as in Hurwitz et al. (2011). Because of the anomalous conditions in the SH stratosphere during the 2002 winter season (i.e., Newman and Nash, 2005), the 2002-2003 WPEN event has been excluded from the present analysis. The observed WPEN and ENSON events considered in the following analysis are listed in Table 1. Three WPEN events are coincident with QBO-E (WPEN/QBO-E) and three are coincident with QBO-W (WPEN/QBO-W). 12 ENSON events are distributed throughout the satellite era.

2.2 A new formulation of the GEOS V2 CCM

The GEOS V2 CCM couples the GEOS-5 general circulation model (GCM) with a comprehensive stratospheric chemistry module (Bloom et al., 2005; Pawson et al., 2008). The model has 2° latitude × 2.5° longitude horizontal resolution and 72 vertical layers, with a model top at 0.01 hPa. Predicted distributions of water vapour, ozone, greenhouse gases (CO_2, CH_4, and N_2O) and CFCs (CFC-11 and CFC-12) feedback to the radiative calculations. The performance of the GEOS V2 CCM was evaluated in detail by SPARC CCMVal (2010). The present study considers a new formulation of the GEOS V2 CCM, with an updated GCM and a new gravity wave drag scheme.

The present version of the GEOS-5 GCM uses the finite-volume dynamics of Lin (2004). Physical parameterizations include schemes for atmospheric convection, large-scale precipitation and cloud cover, longwave and shortwave radiation, turbulence, gravity wave

drag, as well as a land surface model. Convection is parameterized using the Relaxed Arakawa-Schubert (RAS) scheme (Moorthi and Suarez, 1992) and a scheme for the re-evaporation of falling rain (Bacmeister, 2006). RAS is a mass flux scheme with an updraft-only detraining plume cloud model and a quasi-equilibrium closure. The longwave radiative processes are described by Chou et al. (2001), and include absorption due to cloud water, water vapour, carbon dioxide, ozone, N_2O and methane. The shortwave radiative scheme follows Chou and Suarez (1999), and includes absorption by water vapour, ozone, oxygen, CO_2, CH_4, N_2O, CFC-11, CFC-12 and HCFC-22, as well as scattering by cloud water and aerosols. The turbulence parameterization is based on the Lock (2000) scheme, acting together with the Richardson-number based scheme of Louis et al. (1982). The Monin-Obukhov surface layer parameterization is described in Helfand and Schubert (1995). The Koster et al. (2000) land surface model is a catchment-based scheme that defines two soil layers for temperature, three soil layers for moisture, a snow pack and a canopy interception reservoir.

A previous version of the GEOS-5 GCM was used as part of MERRA, as described in Rienecker et al. (in preparation). Major changes to the moisture, turbulence and gravity wave drag schemes were made from this previous model version (Molod et al., in preparation). Increased re-evaporation of grid scale and convective precipitation, along with modifications to the turbulence parameterizations to limit the impact of the Lock scheme and enhance the impact of the Louis scheme in the presence of wind shear, improved the simulated tropical convergence and convection patterns, as well as the global stationary wave patterns. As noted by Hurwitz et al. (2010), the representation of tropospheric stationary wave patterns determines a model's ability to simulate eddy heat flux at 100 hPa.

The model's gravity wave parameterization (GWP) computes the momentum and heat deposition to the breaking of orographic and non-orographic gravity waves using the linear saturation theory by Lindzen (1981). Orographic gravity wave stress is specified using the formulation derived by McFarlane (1987) and given at the top of the subgrid-scale mountains. Subgrid-scale orography is assumed to be horizontally isotropic, and hence the orographic wave stress is oriented opposite to the wind direction averaged below the top of the subgrid mountains. Non-orographic wave stress is given as a Gaussian-shaped phase speed spectrum

at 400 hPa; phase speeds are assumed to be parallel to the wind direction at 400 hPa. The spectrum is composed of 9 waves with ground based phase speeds ranging from –40 to 40 m s^{-1} at an interval of 10 m s^{-1}, as in Garcia and Solomon (1985). As non-orographic gravity waves often accompany precipitation (e.g., convective and frontal systems; see Richter et al., 2010), the latitudinal structure of the gravity wave spectrum is designed to mimic the structure of the climatological mean precipitation field: The spectrum maximizes (7.7×10^{-3} N m^{-2}) at the equator, has two secondary maxima of 2×10^{-3} N m^{-2} at 60°N and 60°S, and is weakest at subtropical latitudes. The tropical peak in non-orographic gravity wave stress is necessary for the generation of an internal QBO in the model (as in Ziemke et al., 2010; see also Section 3.1).

In the Lindzen-based scheme, the horizontal wavelength is 100 km both for orographic and non-orographic waves. A 700 km wavelength is used for the tropical non-orographic waves to prevent an excessive downward propagation of the semi-annual oscillation into the lower stratosphere, and thus contamination of the QBO signal. The intermittency factor is doubled for orographic waves south of the 40°S, based on the observations of strong mountain waves from the Antarctic peninsula (Alexander and Teitelbaum, 2007) and isolated small islands (Alexander et al., 2009). This increased intermittency factor is effective in producing a reasonable evolution of the breakup of the Antarctic vortex.

Heat transfer due to gravity wave breaking is required for the conservation of grid-scale energy across the GWP. Heat transfer is computed from the deposition of the gravity wave energy flux into the mean flow following Warner and McIntyre (2001) and Shaw and Shepherd (2009). In addition, for the conservation of angular momentum and energy, gravity waves stress and energy flux is gradually dissipated in the top five model layers, as suggested by Shaw and Shepherd (2007).

2.3 GEOS V2 CCM simulations

Two, 50-year time-slice simulations with the GEOS V2 CCM will be considered in Section 3. Each simulation is forced by a distinct set of SST and sea ice climatologies, each with a repeating annual cycle, with conditions composited from a number of observed WPEN and

ENSON events (see Table 1). Each event spans from the July preceding the SONDJF peak in tropical SST anomalies through June of the following year. HadISST1 SSTs and sea ice concentrations at 1°x1° resolution (Rayner et al., 2003) are used to prepare the composites. The SSTs used in the WPEN and ENSON simulations are significantly different throughout most of the tropical Pacific.

The set of events used to create the SST and sea ice boundary conditions in the GEOS V2 CCM simulations is slightly different from that used in the MERRA analysis (Table 1). HadISST1 data were not available for the 2008 ENSON and 2009 WPEN events. The 1991 and 1994 WPEN events were associated with large SST anomalies in the central Pacific (Kug et al., 2009) and are thus used to generate a strong model response.

Both simulations used fixed greenhouse gas and ozone-depleting substance boundary conditions representative of the year 2005. Variability related to the solar cycle and volcanic eruptions is not considered.

3 Results

3.1 Climatology of the ENSON simulation

The mean annual cycles of temperature and zonal wind at 60°S, in the ENSON simulation, are shown in Figure 1. The GEOS V2 CCM (Figure 1c) is generally able to simulate the observed stratospheric temperature pattern (Figure 1a). As has been noted in evaluations of earlier formulations of this model (Pawson et al., 2008; SPARC CCMVal, 2010), polar stratospheric temperatures are biased high in the lower stratosphere in mid-winter. Similarly, the model is broadly able to simulate the SH polar jet. Modelled winds (Figure 1d) remain weaker than observed (Figure 1b) in the middle stratosphere, in mid- to late winter. The simulation of the breakup of the Antarctic vortex is comparable to that reported by Hurwitz et al. (2010).

A timeseries of zonal winds in the equatorial region, in 10 years of the ENSON simulation, is shown in Figure 2b. The MERRA timeseries of zonal winds in the 1990s is shown for

comparison (Figure 2a). The modelled QBO has a realistic period (30 ± 3 months, at 30 hPa) though the descent of easterly and westerly anomalies from the upper stratosphere is slower than observed. The modelled QBO amplitude is well simulated around 10 hPa but is weaker than observed in the lower stratosphere. Note that the QBO signal is absent at 50 hPa: zonal winds are generally easterly. For this reason, 30 hPa zonal winds in the 10°S-10°N region are used to characterize the phase of the modelled QBO. As for the MERRA reanalysis, QBO-E years are identified when the modelled November/December mean QBO index is less than -2 m s^{-1} while QBO-W years are identified when the QBO index is larger than 2 m s^{-1}. For each simulation, there are approximately 25 years designated as QBO-E and 15 years designated as QBO-W.

3.2 Stratospheric response to WPEN events

October/November eddy heat flux at 40-80°S, 100 hPa is a measure of the planetary wave energy entering the SH polar stratosphere (Newman et al., 2001). In the MERRA reanalysis (see Table 2), eddy heat flux in the WPEN/QBO-E composite is significantly different than that in all three of the other composites at the 95% confidence level, in a two-tailed t-test with unequal variance. Though October/November eddy heat flux in the GEOS V2 CCM (Table 2) is weaker than observed, the model is able to capture some of the observed variability. For example, eddy heat flux values in the WPEN/QBO-W and ENSON/QBO-W composites are different at the 90% level. Differences between the modelled WPEN/QBO-E and WPEN/QBO-W composites are not statistically significant. As in the MERRA reanalysis, the magnitude of the eddy heat flux in the ENSON simulation does not depend on the phase of the QBO.

Enhanced eddy heat flux in October/November is associated with a warming of the Antarctic lower stratosphere in November/December (Hurwitz et al., 2011). In MERRA, the Antarctic lower stratosphere warms 3-5 K in response to WPEN events in November/December (Figure 3a), while the upper stratosphere cools by approximately 1 K. In the Antarctic lower stratosphere, the QBO-related temperature response during WPEN (Figure 3b) is nearly identical to the WPEN response itself: a 4-5 K warming that is significantly different from zero at the 95% confidence level. That is, this warming signal can be attributed to WPEN/QBO-E events.

The GEOS V2 CCM is able to simulate the observed Antarctic temperature response to WPEN events, but not the modulation of this response by the QBO. November/December temperature differences between the WPEN and ENSON simulations, during QBO-E, are approximately 2-4 K in the lower stratosphere with a roughly 1 K cooling response above 10 hPa (Figure 3c). Figure 3d shows that the modelled temperature response to WPEN is insensitive to the phase of the QBO: the lower stratosphere warms in both QBO-E and QBO-W years.

3.3 Tropospheric response to WPEN events

Several tropospheric diagnostics are used to investigate the model's insensitivity to the phase of the QBO: differences in OLR, the upper tropospheric streamfunction and calculations of Rossby wave energy in the tropical and subtropical south Pacific. As discussed by Hurwitz et al. (2011), SON seasonal mean upper tropospheric streamfunction differences illustrate the planetary wavetrains generated in response to El Niño events. Figure 4 compares the 250 hPa streamfunction in the WPEN versus ENSON cases, as well differences between QBO-E and QBO-W during WPEN events. In the MERRA reanalysis, southeastward-propagating wavetrains are seen in response to both WPEN (Figure 4a) and the QBO (Figure 4b). The model simulates the wavetrain response to WPEN (Figure 4c), with comparable magnitude and propagation direction, but lacks sensitivity to the phase of the QBO (Figure 4d).

Vera et al. (2004) identified a planetary wave source region in the south central Pacific, during austral spring, in WPEN-like events as compared with cold tongue El Niño and ENSO neutral events. The authors determined that the increase in planetary wave activity was the result of enhanced upper level divergence. That is, enhanced convection in the south central Pacific leads to an enhancement in Rossby wave activity and thus to a stronger poleward-propagating wavetrain in the SH. In Figure 5, OLR differences illustrate changes in convection in MERRA and in the GEOS V2 CCM simulations. Negative OLR differences imply relatively higher cloud tops and thus deeper convection. Figures 5a and 5c show the convective response to WPEN events, during QBO-E. The largest OLR differences in Figures 5a and 5c occur in the equatorial region, and are associated with well-established

ENSO-related longitudinal shifts in convection. The convective response to WPEN events extends to the SH subtropics: there are negative OLR differences in the Rossby wave source region identified by Vera et al. (red boxes) in both the NOAA interpolated OLR dataset (Figure 5a) and in the model simulations (Figure 5c).

In MERRA, there is a distinct region of negative OLR differences in the Rossby wave source region in response to the QBO, during WPEN events (Figure 5b). This result suggests that QBO-related changes in tropical circulation modulate the depth of convective activity in the subtropics, consistent with the hypothesis of Collimore et al. (2003). In contrast, there are no significant differences in OLR in this region in the model (Figure 5d).

Similarly, in the MERRA reanalysis and during the SON season, Rossby wave source calculations (based on Jin and Hoskins, 1995) show increases in the Vera et al. (2004) planetary wave source region (red boxes) in WPEN events relative to ENSON (Figure 6a) and WPEN/QBO-E relative to WPEN/QBO-W (Figure 6b). In the GEOS CCM, there is a relative Rossby wave source in the central Pacific south of 20°S during WPEN events (Figure 6c); however, this response lacks sensitivity to the phase of the QBO (Figure 6d). Possible reasons for the model's lack of sensitivity to the QBO phase will be discussed in Section 4.

4 Summary and discussion

WPEN is an emerging type of El Niño event (Kug et al., 2009). CCMs used to predict ozone recovery and the 21st century stratospheric climate need to capture the extra-tropical stratospheric response to WPEN, since these events are predicted to occur more frequently in future (Yeh et al., 2009; Xie et al., 2010).

This study was the first to examine the modelled response of the Antarctic stratosphere to WPEN, as well as the modulation of this response by the QBO. Two time-slice simulations, one representing WPEN conditions and the other ENSON conditions, were used to both test a new formulation of the GEOS V2 CCM and confirm the observed atmospheric response to

recent WPEN events (as described by Hurwitz et al., 2011). The MERRA reanalysis was used to validate the modelled response to WPEN.

WPEN events enhanced poleward planetary wave activity in the central South Pacific during austral spring. In both MERRA and in the GEOS V2 CCM, enhanced eddy heat flux hastened the breakup of the Antarctic vortex by approximately 5 days at 60°S, 10 hPa and led to a relative warming of the Antarctic lower stratosphere in November/December. During QBO-E, the GEOS V2 CCM simulated a warming of 2-4 K in the Antarctic lower stratosphere, in the WPEN simulation relative to ENSON. The modelled temperature response to WPEN events had the same vertical and meridional structure but was somewhat weaker than that in the MERRA reanalysis (4-5 K). The relatively weaker model response is likely a consequence of the experimental design: This study compared the transient atmospheric response (i.e., in the MERRA reanalysis) with time-slice simulations, each representing a near-equilibrium climate.

Analysis of MERRA demonstrated the sensitivity of the WPEN response to the phase of the QBO, in the 1979-2009 period. The lower stratospheric WPEN-related warming signal was as large as the QBO-related warming signal, suggesting that this signal could be attributed to WPEN events coincident with the easterly phase of the QBO. Tropospheric diagnostics suggest that it is the combination of the placement of convective activity in the subtropical Pacific during WPEN events, and the enhancement of this convective activity during QBO-E, that lead to changes in planetary wave activity in the SH and thus to the stratospheric temperature response.

In the GEOS V2 CCM simulations, the Antarctic temperature response to WPEN events was insensitive to the phase of the QBO. OLR, streamfunction and Rossby wave source diagnostics demonstrated that the modelled QBO did not extend far enough into the lower stratosphere and upper troposphere to modulate convection and thus planetary wave activity in the south central Pacific. In the model formulation examined in this study, zonal winds in the lower stratosphere (i.e., 50 hPa) were almost always easterly, regardless of the phase of the QBO at higher altitudes (i.e., 30 hPa). Thus, the model produced an easterly QBO-like

response to WPEN in both phases of the middle stratospheric QBO. If the QBO westerly anomalies were to descend further into the lower stratosphere and/or or upper troposphere, better matching observations, the model would likely be able to simulate QBO-related modulation of subtropical convection and in turn the dependence of the WPEN response on the QBO phase.

Acknowledgements

The authors thank C. I. Garfinkel for the Rossby wave source calculations and NASA's MAP program for funding. M. M. Hurwitz is supported by an appointment to the NASA Postdoctoral Program at Goddard Space Flight Center, administered by Oak Ridge Associated Universities through a contract with NASA.

References

Alexander, M. J., and Teitelbaum, H.: Observation and analysis of a large amplitude mountain wave event over the Antarctic peninsula, J. Geophys. Res., 112, D21103, doi:10.1029/2006JD008368, 2007.

Alexander, M. J., Eckermann, S. D., Broutmann, D., and Ma, J.: Momentum flux estimates for South Georgia Island mountain waves in the stratosphere observed via satellite, Geophys. Res. Lett., 36, L12816, doi:10.1029/2009GL038587, 2009.

Ashok, K., Behera, S. K., Rao, S. A., Weng, H., and Yamagata, T.: El Niño Modoki and its possible teleconnections, J. Geophys. Res., 112, C11007, doi:10.1029/2006JC003798, 2007.

Bacmeister, J. T., Suarez, M. J., and Robertson, F. R.: Rain re-evaporation, boundary-layer/convection interactions and Pacific rainfall patterns in an AGCM, J. Atmos. Sci., 63, 3383-3403, 2006.

Bosilovich, M.: NASA'S modern era retrospective-analysis for research and applications: integrating earth observations, Earthzine, Sep. 26, 2008.

Bloom, S., da Silva, A., Dee, D., Bosilovich, M., Chern, J.-D., Pawson, S., Schubert, S., Sienkiewicz, M., Stajner, I., Tan, W.-W., Wu, M.-L.: Documentation and validation of the Goddard Earth-Observing System (GEOS) Data Assimilation System Version 4, Tech. Rep. 104606, V26, NASA, Greenbelt, Maryland, 2005.

Bronnimann, S., Luterbacher, J., Staehelin, J., Svendby, T. M., Hansen, G., and Svene, T.: Extreme climate of the global troposphere and stratosphere in 1940-42 related to El Niño, Nature, 431, 971-974, doi:10.1038/nature02982, 2004.

Cagnazzo, C., Manzini, E., Calvo, N., Douglass, A., Akiyoshi, H., Bekki, S., Chipperfield, M., Dameris, M., Deushi, M., Fischer, A. M., Garny, H., Gettelman, A., Giorgetta, M. A., Plummer, D., Rozanov, E., Shepherd, T. G., Shibata, K., Stenke, A., Struthers, H., Tian, W.: Northern winter stratospheric temperature and ozone response to ENSO inferred from an ensemble of Chemistry Climate Models, Atmos. Chem. Phys., 9, 8935-8948, 2009.

Chou, M.-D., and Suarez, M. J.: A Solar Radiation Parameterization for Atmospheric Studies, NASA Technical Report Series on Global Modeling and Data Assimilation 104606, v15, 40 pp, 1999.

Chou, M.-D., Suarez, M. J., Liang, X. Z., and Yan, M. M.-H.: A Thermal Infrared Radiation Parameterization for Atmospheric Studies, NASA Technical Report Series on Global Modeling and Data Assimilation 104606, v19, 56 pp, 2001.

Collimore, C. C., Martin, D. W., Hitchman, M. H., Huesman, A., and Waliser, D. E.: On the relationship between the QBO and tropical deep convection, J. Climate, 16, 2552-2568, 2003.

Free, M., and Seidel, D. J.: Observed El Niño-Southern Oscillation temperature signal in the stratosphere, J. Geophys. Res., 114, D23108, doi:/10.1029/2009JD012420, 2009.

Garcia, R. R., and Solomon, S.: The effect of breaking gravity waves on the dynamics and chemical composition of the mesosphere and lower thermosphere, J. Geophys. Res., 90, 3850–3868, 1985.

Garfinkel, C. I., and Hartmann, D. L.: Effects of the El Niño-Southern Oscillation and the Quasi-Biennial Oscillation on polar temperatures in the stratosphere, J. Geophys. Res., 112, D19112, doi:10.1029/2007JD008481, 2007.

Garfinkel, C. I., and Hartmann, D. L.: Different ENSO teleconnections and their effects on the stratospheric polar vortex, J. Geophys. Res., 113, D18114, doi:10.1029/2008JD009920, 2008.

Helfand, H. M., and Schubert, S. D.: Climatology of the simulated Great Plains low-level jet and its contribution to the continental moisture budget of the United States, J. Climate, 8, 784-806, 1995.

Hurwitz, M. M., Newman, P. A., Li, F., Oman, L. D., Morgenstern, O., Braesicke, P., and Pyle, J. A.: Assessment of the breakup of the Antarctic polar vortex in two new chemistry-climate models, J. Geophys. Res., 115, D07105, doi:10.1029/2009JD012788, 2010.

Hurwitz, M. M., Newman, P. A., Oman, L. D., and Molod, A. M.: Response of the Antarctic Stratosphere to two Types of El Niño events, J. Atm. Sci., in press, 2011.

Jin, F.-F., and Hoskins, B. J.: The direct response to tropical heating in a baroclinic atmosphere, J. Atm. Sci., 52, 307-319, 1995.

Koster, R. D., Suarez, M. J., Ducharne, A., Stieglitz, M., and Kumar, P.: A catchment-based approach to modeling land surface processes in a GCM, Part 1, Model Structure, J. Geophys. Res., 105, 24809-24822, 2000.

Kug, J.-S., Jin, F.-F., and An, S.-I.: Two types of El Nino events: cold tongue El Niño and warm pool El Niño, J. Climate, 22, 1499-1515, 2009.

Larkin, N. K., and Harrison, D. E.: On the definition of El Niño and associated seasonal average U.S. weather anomalies, Geophys. Res. Lett., 32, L13705, doi:10.1029/2005GL022738, 2005.

Liebmann, B., and Smith, C. A.: Description of a complete (interpolated) outgoing longwave radiation dataset, Bulletin of the American Meteorological Society, 77, 1275-1277, 1996.

Lin, S.-J.: A vertically Lagrangian finite-volume dynamical core for global models, Mon. Wea. Rev., 132, 2293-2307, 2004.

Lindzen, R. S.: Turbulence and stress owing to gravity wave and tidal breakdown, J. Geophys. Res., 86, 9707–9714, 1981.

Lock, A. P., Brown, A. R., Bush, M. R., Martin, G. M., and Smith, R. N. B.: A new boundary layer mixing scheme. Part I: Scheme description and single-column model tests, Mon. Wea. Rev., 138, 3187-3199, 2000.

Louis, J., Tiedtke, M., and Geleyn, J.: A short history of the PBL parameterization at ECMWF, Proc. ECMWF Workshop on Planetary Boundary Layer Parameterization, Reading, United Kingdom, ECMWF, 59-80, 1982.

Manzini, E., Giorgetta, M. A., Esch, M., Kornblueh, L., and Roeckner, E.: The influence of sea surface temperatures on the Northern winter stratosphere: ensemble simulations with the MAECHAM5 model, J. Climate, 19, 3863-3881, 2006.

McFarlane, N. A.: The effect of orographically excited gravity-wave drag on the circulation of the lower stratosphere and troposphere, J. Atmos. Sci., 44, 1775–1800, 1987.

Molod, A. M., et al.: Climate simulations with the GEOS-5 AGCM: Transition from MERRA to AR5, in preparation.

Moorthi, S., and Suarez, M. J.: Relaxed Arakawa-Schubert, A Parameterization of Moist Convection for General-Circulation Models, Mon. Wea. Rev., 120, 978-1002, 1992.

Newman, P. A., and Nash, E. R.: The unusual Southern Hemisphere stratosphere winter of 2002, J. Atm. Sci., 62, 614-626, 2005.

Newman, P. A., Nash, E. R., and Rosenfield, J. E.: What controls the temperature of the Arctic stratosphere during the spring?, J. Geophys. Res., 106, D17, 19,999-20,010, 2001.

Pawson, S., Stolarski, R. S., Douglass, A. R., Newman, P. A., Nielsen, J. E., Frith, S. M., and Gupta, M. L.: Goddard Earth Observing System chemistry-climate model simulations of stratospheric ozone-temperature coupling between 1950 and 2005, J. Geophys. Res., 113, D12103, doi:10.1029/2007JD009511, 2008.

Rasmusson, E. M., and Carpenter, T. H.: Variation in tropical sea surface temperature and surface wind fields associated with Southern Oscillation/El Niño, Mon. Weather Rev., 110, 354-384, 1982.

Rayner, N. A., Parker, D. E., Horton, E. B., Folland, C. K., Alexander, L. V., Rowell, D. P., and Kaplan, A.: Global analyses of sea surface temperature, sea ice, and night marine air temperature since the late nineteenth century, J. Geophys. Res., 108, D14, 4407, 2003.

Richter, J. H., Sassi, F., and Garcia, R. R.: Toward a physically based gravity wave source parameterization in a general circulation model, J. Atmos. Sci., 67, 136–156, 2010.

Rienecker, M. M., et al.: MERRA - NASA's Modern-Era Retrospective Analysis for Research and Applications, in preparation.

Sassi, F., Kinnison, D., Boville, B. A., Garcia, R. R., and Roble, R.: Effect of El Niño-Southern Oscillation on the dynamical, thermal, and chemical structure of the middle atmosphere, J. Geophys. Res., 94, 14705-14716, doi:10.1029/JD094iD12p14705, 2004.

Shaw, T. A., and Shepherd, T. G.: Angular momentum conservation and gravity wave drag parameterization: Implications for climate models, J. Atmos. Sci., 64, 190–203, 2007.

Shaw, T. A., and Shepherd, T. G.: A theoretical framework for energy and momentum consistency in subgrid-scale parameterization for climate models, J. Atmos. Sci., 66, 3095–3114, 2009.

SPARC CCMVal: SPARC Report on the Evaluation of Chemistry-Climate Models, V. Eyring, T. G. Shepherd, D. W. Waugh (Eds.), SPARC Report No. 5, WCRP-132, WMO/TD-No. 1526, http://www.atmosp.physics.utoronto.ca/SPARC, 2010.

Vera, C., Silvestri, G., Barros, V., and Carril, A.: Differences in El Niño response over the Southern Hemisphere, J. Climate, 17, 1741-1753, 2004.

Warner, C. D., and McIntyre, M. E.: An ultrasimple spectral parameterization for nonorographic gravity waves, J. Atmos. Sci., 58, 1837–1857, 2001.

Xie, S.-P., Deser, C., Vecchi, G. A., Ma, J., Teng, H. Y., and Wittenberg, A. T.: Global warming pattern formation: sea surface temperature and rainfall, J. Climate, 23, 966-986, 2010.

Yeh, S.-W., Yim, B. Y., Noh, Y., and Dewitte, B.: Changes in mixed layer depth under climate change projections in two CGCMs, Climate Dynamics, 33, 199–213, 2009.

Ziemke, J. R., Chandra, S., Oman, L. D., and Bhartia, P. K.: A new ENSO index derived from satellite measurements of column ozone, Atmos. Chem. Phys., 10, 3711-3721, 2010.

Table 1. List of ENSO events composited to create the SST and sea ice boundary conditions for the WPEN and ENSON simulations. The years shown refer to the SON season included for each event. * symbols denote QBO-E years; ^ symbols denote QBO-W years.

	MERRA Composites	**Events Composited to Create Boundary Conditions for GEOS CCM Simulations**
WPEN	1986 1991* 1994* 2003* 2004^ 2006^ 2009^	1991* 1994*
ENSON	1979* 1980^ 1981* 1985^ 1989* 1992* 1993^ 1996* 2000 2001* 2005* 2008^	1979* 1980^ 1981* 1985^ 1989* 1992* 1993^ 1996* 2001* 2005*

Table 2. October/November mean eddy heat flux magnitude (K m s^{-1}) at 40-80°S, 100 hPa ± 2 standard deviations.

ENSO Composite	QBO Phase	MERRA	GEOS CCM
WPEN	**E**	16.64 ± 5.09	7.11 ± 2.27
	W	10.22 ± 2.38	7.86 ± 4.65
ENSON	**E**	11.12 ± 3.69	6.54 ± 3.10
	W	11.79 ± 2.36	6.49 ± 3.54

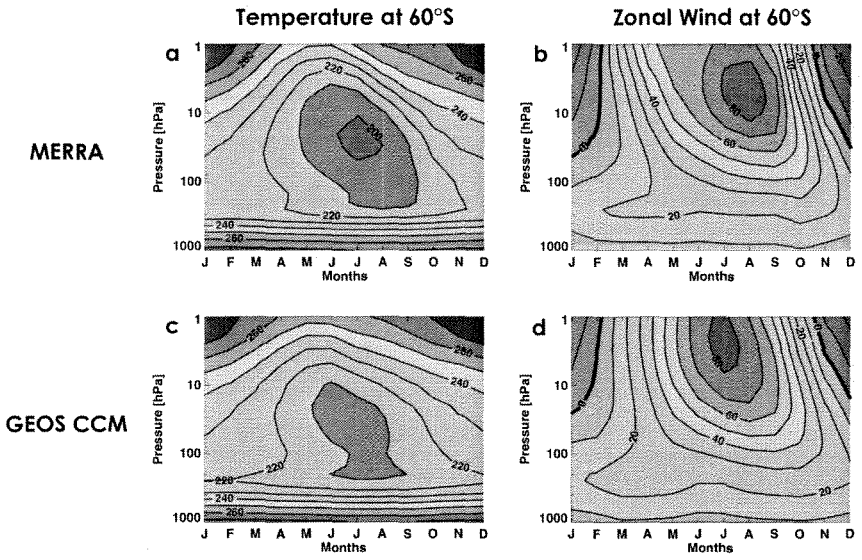

Figure 1. Temperature (K) (a, c) and zonal wind (m s^{-1}) (b, d) at 60°S, as a function of month and altitude, in (a, b) a composite of ENSO neutral years in the MERRA reanalysis and (c, d) the ENSON simulation.

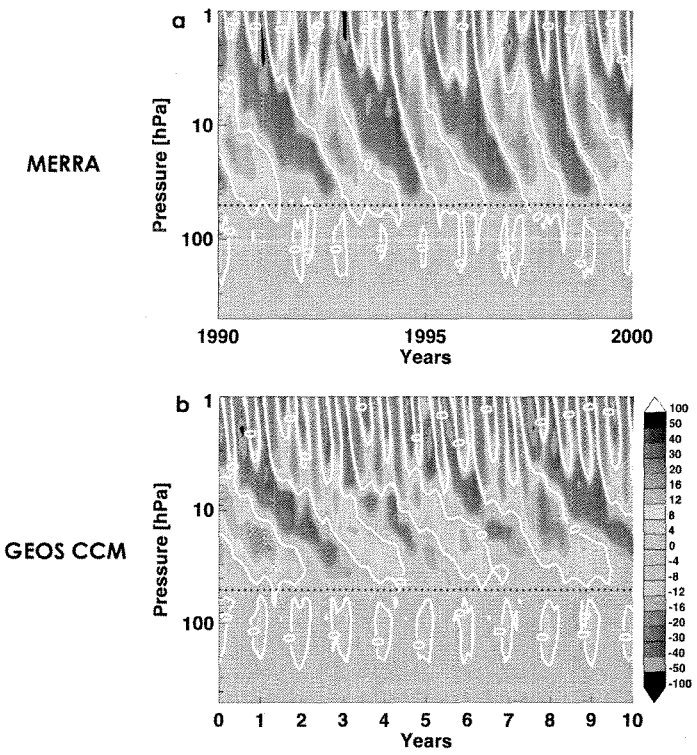

Figure 2. Equatorial (4°S-4°N) zonal mean zonal wind (m s^{-1}), as a function of time and altitude: (a) 1990 through 1999 in MERRA; (b) 10 years of the ENSON simulation. White contours denote the zero wind line. The black dotted line highlights the 50 hPa level.

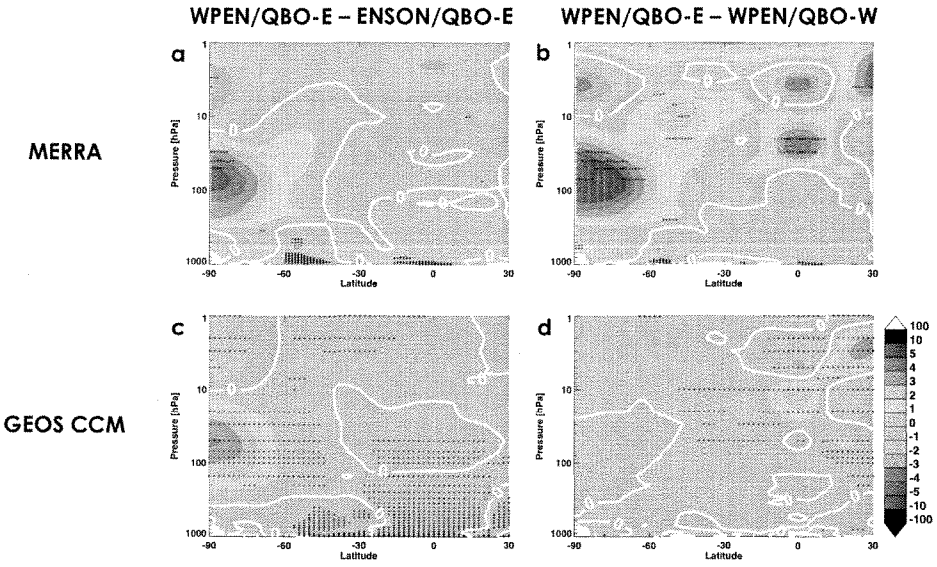

Figure 3. November/December temperature differences (K) in (a, b) MERRA and (c, d) the GEOS CCM simulations. The response to WPEN events during QBO-E is shown in (a) and (c). The response to the QBO phase during WPEN events is shown in (b) and (d). White contours indicate zero difference. Black Xs indicate regions where differences are significant at the 95% confidence level.

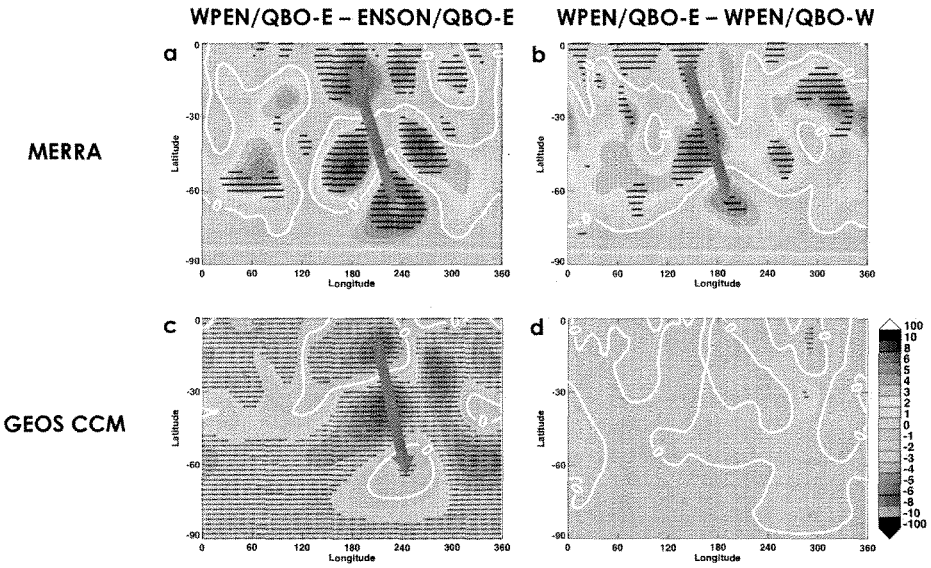

Figure 4. Longitude-latitude contour plots showing SON seasonal mean streamfunction differences at 250 hPa (10^{-6} m^3 s^{-1}) in (a, b) NCEP and (c, d) the GEOS CCM simulations. The response to WPEN events during QBO-E is shown in (a) and (c). The response to the QBO phase during WPEN events is shown in (b) and (d). White contours indicate zero difference. Black Xs indicate regions where differences are significant at the 90% confidence level in the MERRA reanalysis and 95% confidence level in the GEOS CCM. Red arrows indicate the approximate direction of planetary wave propagation.

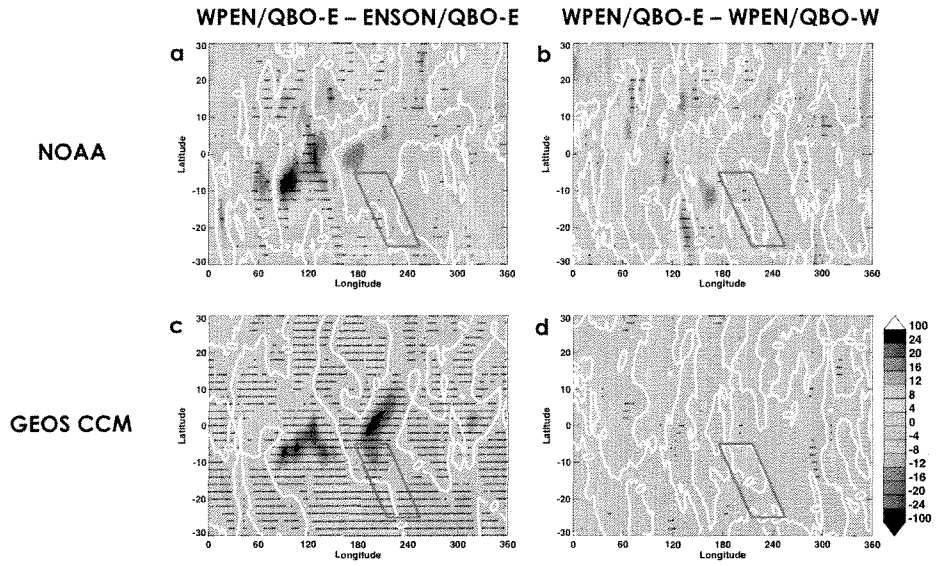

Figure 5. Longitude-latitude contour plots showing SON seasonal mean OLR differences (W m^{-2}) in (a, b) NOAA and (c, d) the GEOS CCM simulations. The response to WPEN events during QBO-E is shown in (a) and (c). The response to the QBO phase during WPEN events is shown in (b) and (d). White contours indicate zero difference. Black Xs indicate regions where differences are significant at the 90% confidence level in the NOAA interpolated OLR dataset and 95% confidence level in the GEOS CCM. Red boxes indicate the approximate Rossby wave source region found by Vera et al. (2004).

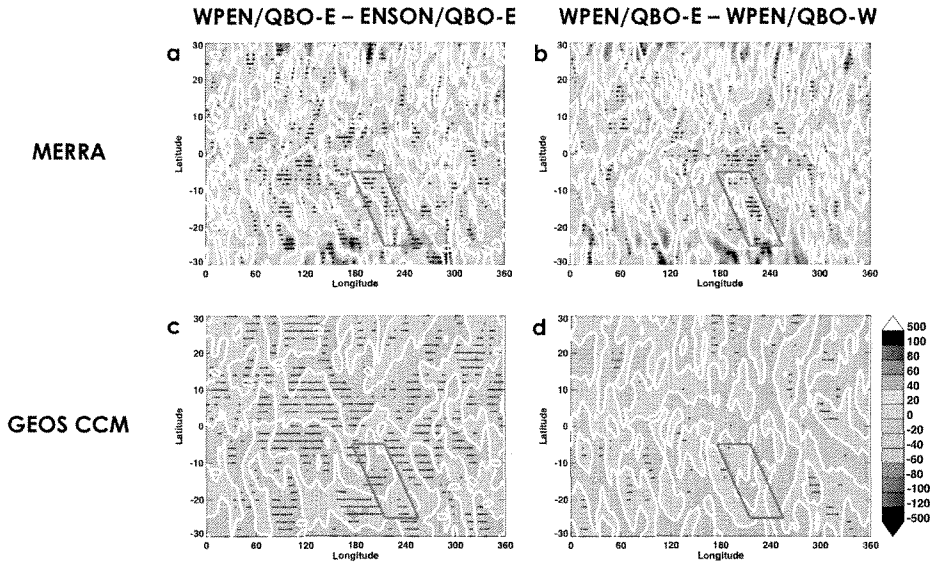

Figure 6. Longitude-latitude contour plots showing SON seasonal mean differences in the Rossby wave source (10^{10} s^{-2}), as described in the text, in (a, b) MERRA and (c, d) the GEOS CCM simulations. The response to WPEN events during QBO-E is shown in (a) and (c). The response to the QBO phase during WPEN events is shown in (b) and (d). White contours indicate zero difference. Black Xs indicate regions where differences are significant at the 95% confidence level. Red boxes indicate the approximate Rossby wave source region found by Vera et al. (2004).